RESEARCH ARTICLE

Preparation of highly sensitive flexible bending sensors and their application in human motion monitoring

Yu Shao[1], Xiaozhou Huang[2], Ming Lv[3, *]

[1]School of Physical Education, Shanghai University of Sport, Shanghai, China. [2]Physical Education Teaching and Research Group, Changsha Foreign Languages School, Changsha, Hunan, China. [3]Department of Public Basic Education, Anhui Technical College of Mechanical and Electrical Engineering, Wuhu, Anhui, China.

Received: January 20, 2025; **accepted:** May 9, 2025.

Flexible bending sensors serve as a crucial interface between humans and smart devices. It can monitor human motion to assess individual health status and exercise performance, which helps to better understand and distribute human health related data. It can also provide more reliable prediction results and decision support. To prepare a high-sensitivity flexible bending sensor for human body motion monitoring, polyimide film was used as the encapsulation material. The "polyimide film-sensor-polyamide hot melt adhesive film-polyimide film" structure was constructed by utilizing the excellent adhesion of polyamide hot melt adhesive film. The adhesion was realized by heat pressing at 130°C for 20 s, and the stability of the sensor resistance value was verified in cyclic bending test at 110° for 10 times with an error of no more than 2 Ω. The results showed that the prepared sensors exhibited high sensitivity and responsiveness at different bending angles with a minimum resolution of 0.5°, which accurately captured the dynamic changes. In addition, the output voltage changes of the sensor increased from 0.00087 V to 0.01002 V under strains from 0.5 to 4.0°. The sensitivity ranged from 1.74 to 2.50 V/°, and the response time decreased from 120 ms to 85 ms, showing good repeatability and stability. This study developed a novel flexible sensor type with excellent sensitivity and stability for motion tracking, which could be used in motion analysis and health monitoring.

Keywords: high sensitivity; flexible bending sensor; motion monitoring; polyimide film; polyamide hot melt adhesive film; resistive stability.

[*]**Corresponding author:** Ming Lv, Department of Public Basic Education, Anhui Technical College of Mechanical and Electrical Engineering, Wuhu 241002, Anhui, China. Email: lvming2023@126.com.

Introduction

Flexible bending sensors have drawn a lot of attention in research and application due to the quick growth of wearable technology and the Internet of Things as they serve as a crucial interface between humans and smart devices [1]. The need for flexible sensors with high accuracy and sensitivity is increasing in the domains of motion analysis, virtual reality, and health monitoring [2]. Current research has shown that the monitoring of human motion is important for assessing individual health status, improving exercise performance, and rehabilitating medical treatment [3]. However, traditional flexible sensors have many shortcomings in practical applications such as unstable performance under extreme temperature or humidity conditions, poor mechanical durability, and insufficient sensitivity and resolution in complex motion monitoring [4]. In traditional studies, the preparation of sensors often relies on complex photolithographic or chemical etching processes, which not only increases the cost but also limits their application in mass production [5]. In addition, the comfort and adaptability of existing sensors for long-term wear are limited. Especially in dynamic human motion monitoring, it is still a technical challenge to accurately capture subtle changes in motion [6].

In several studies in the field of flexible sensor, innovative design and high sensitivity detection techniques have been widely used to promote the development of electronic skin, intelligent robotics, and human-computer interaction. Yang *et al*. prepared a tin selenide/multi-walled carbon nanotube pressure sensor with a geometric spine microstructure through a bionic strategy. A flexible inter-finger electrode, a tin selenide/multi-walled carbon nanotube sensitive film, and a micropatterned polydimethylsiloxane substrate made up the sensor's structure. It could achieve a high sensitivity of 165/kPa in the range of 0 - 80 kPa as well as a fast response time of 88 ms. The results demonstrated good detection capability and was suitable for human movement and health signal monitoring [7]. Xi *et al*. developed a multimodal flexible tactile sensor based on a polypyrrole/$Ti_3C_2T_x$ sensitive thin film with the ability to detect humidity and pressure simultaneously. The sensor reached a sensitivity of 89,113.4 Ω/% RH in the range of 0 - 97% RH with response times of 2.5 s for humidity and 67 ms for tactile pressure, which exhibited excellent stability and repeatability and was suitable for breathing patterns and motion detection [8]. Pan *et al*. addressed the application of flexible humidity sensors for respiratory monitoring with sensors prepared using near-field electrohydrodynamic direct-write technology. The ability to monitor effectively under a wide range of respiratory conditions demonstrated its potential in health monitoring [9]. A printed porous conductive composite made of carbon black and polydimethylsiloxane was created by Wang *et al*., which enabled the sensor to show multifunctional application potential for human motion and directional motion detection of soft robot gripper jaws. The sensor achieved high bi-directional sensitivity and excellent durability through deep eutectic solvent-induced phase separation [10]. Ying *et al*. fabricated high-performance flexible pressure sensors that combined self-assembly technology with good tactility and high sensitivity, which could effectively monitor small deformations and finger bending signals for wearable medical devices and smart robots [11].

The trimethylchloromethylammonium-cadmium chloride (TMCM-$CdCl_3$/PDMS) composites synthesized by Gong *et al*. exhibited high voltage electrical properties. Its power density was as high as 115.2 μW/cm², which could realize the dual functions of energy harvesting and subtle body posture change sensing in self-powered flexible wearable devices [12]. Park *et al*. developed a high tensile strain sensor using thermally induced shrinkage to form a dense nano- to micrometer-scale structure that had a dynamic range of more than 700%, exhibited excellent tensile properties, and was suitable for use as a skin-attached sensor [13]. Li *et al*. were able to create nano dopamine-reinforced hemicellulose-based hydrogels with fast drug release and self-monitoring properties that held up well during cyclic compression and could serve as a foundation for the creation of flexible materials for future drug self-administration and health monitoring [14]. Lu *et al*. developed a multifunctional strain sensor based on the elasticity of knitted fabric to address the durability of smart e-textiles, which possessed good operating range and stability and was suitable for joint monitoring, medical assessment, and gesture recognition [15]. Further, Li *et al*. developed an electrospun nanofiber haptic sensor. The added barium titanate had a positive impact on improving the electrical properties of polyvinylidene fluoride, allowing it to achieve accurate recognition of human movement in health monitoring [16].

Many researchers have studied structural design, material selection, and sensitivity optimization of flexible sensors. However, the current research still suffers from the shortcomings such as insufficient adaptability, response delay in complex movements, and stability of the manufacturing process. Therefore, this study proposed a high-sensitivity flexible bending sensor based on transparent polyimide (PI) film and polyamide (PA) hot melt adhesive film by sandwiching one layer of PA hot melt adhesive film with two layers of PI film to enhance the durability and responsiveness of the sensor. Meanwhile, micropatterning and bionic design were used to improve the adaptability of the sensor under different finger motion states, ensuring that it was capable of high-precision dynamic monitoring in a variety of motion scenarios. This new design was expected to contribute to the future applications of wearable devices in health monitoring, motion tracking, and human-computer interaction.

Materials and methods

Structure and resistance characterization of flexible bending sensor

In the development of the high-sensitivity flexible bending sensor, a chemically and mechanically stable polyimide film was selected as the encapsulation material, and polyamide was used to ensure good adhesion. The PI film was made of PL450C thermoplastic polyimide resin (Mitsui Chemicals Inc., Tokyo, Japan) and was produced by a biaxial stretching process. The PA hot melt adhesive film was made of Zytel series nylon 66 resin (DuPont, Wilmington, DE, USA) and was supplied by Suzhou Zhongsi Cheng New Material Co., Ltd. (Kunshan, Jiangsu, China). In the preparation of high-sensitivity flexible bending sensor, a modified polyester fiber bundle (Lanjing Water Purification Material Factory, Gongyi City, Henan Province) with a diameter of about 300 microns was used as the core sensing material and was surface hydroxylated to enhance hydrophilicity, which provided excellent flexibility and pressure-sensitive properties. The sensor structure consisted of two layers of 0.020 mm thick PI film sandwiched by one layer of 0.08 mm thick PA, forming a "PI-sensor-PA-PI" configuration. Bonding of the PI was achieved by heat pressing at 130°C for 22 s using XINMAIDE 105 four-column hydraulic hot presser (Dongguan Fangtian Machinery Equipment Co., Ltd., Dongguan, Guangdong, China) with an intelligent proportional integral derivative (PID) temperature control system, which ensured simplicity and cost-effectiveness of the package. The sensor was designed in the form of loops and mounted on a flexible printed circuit board to enhance fitness and stability. In the preparation process, conductive paste was obtained by mixing conductive fillers and aqueous polyurethane dispersion (PUD) compounded with Desmodur® XP 2655 waterborne hardener and Bayhydrol® U 4150 polyol (Covestro, Leverkusen, Germany). The viscosity was then adjusted to form a paste suitable for coating and impregnation. The sensing layer was placed between a double-layer encapsulation consisting of PI and PA at the bottom and a single layer of PI at the top. This encapsulation was designed to protect the sensing layer and to improve the environmental resilience and durability of the sensor [17] (Figure 1).

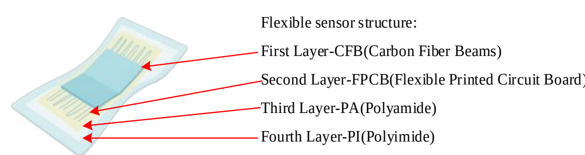

Figure 1. The structure of the flexible bending sensor.

Before constructing the model, the flow of current inside the sensor and its effect on the mechanism was investigated. In the design of the high-sensitivity flexible bending sensor, the electronic components were represented as rectangles with the ends labeled as positive (+) and negative (-). The movement of the electronic component was simplified by an equivalent model in which the yellow arrow indicated its direction of movement during bending. This type of electronic element was capable of accurately detecting small deformations in the bending sensor and converting them into electrical signals, which helped to achieve highly sensitive detection. To improve sensitivity, the study selected fine candidate fiber bundles to improve the detection of small deformations. The current path was optimized to sensitively capture resistance changes. The quantum tunneling effect (QTE) was enhanced to make the resistance change more significant. Moreover, the sensitivity and stability were improved by reducing external interference through double-layer encapsulation. Since the endpoints of current inflow and outflow into and out of the carbon fiber bundle did not affect the mechanism effect, the electron motion path follows a K-type structure. The electrons moved from a starting point perpendicular to the electrode to the electrode below. Further qualitative analysis decomposed the electron movement into two parts including horizontal conduction and vertical tunneling [18]. Radial tunneling occurred in the contact region of the two carbon fiber bundles, where the resistance change was not only affected by the QTE but also related to the size of the contact area (Figure 2).

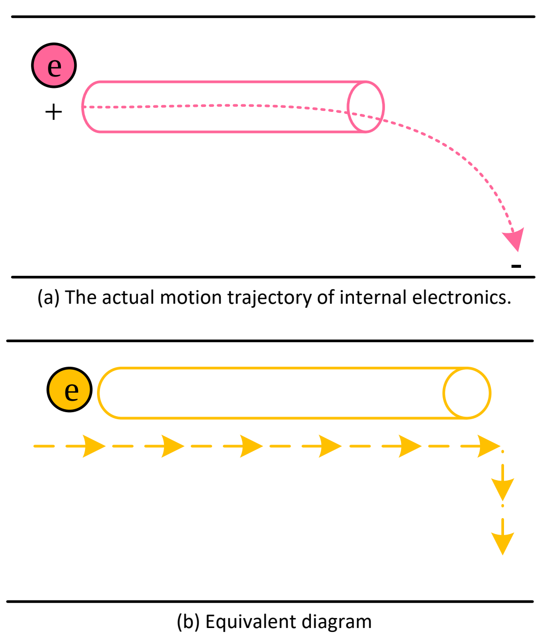

Figure 2. Internal electronic motion direction of bending sensor.

The internal structure of the bending sensor was shown in Figure 3. The parameters of bending sensor cross-section included contact length (a), bundle width (b), vertical height (bundle thickness) (h), contact angle (π+θ), and the horizontal distance (d) between the carbon fiber bundles (Figure 3A). Since h was much smaller than a, the contact portion could be regarded as a rectangle, and a simplified diagram of it was displayed in Figure 3B.

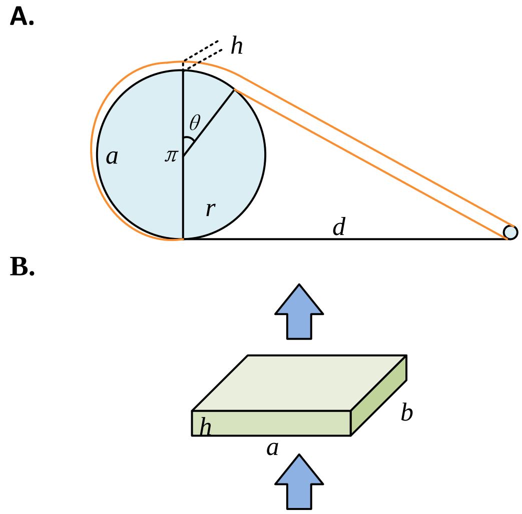

Figure 3. The internal structure of the bending sensor. **A.** Cross sectional schematic diagram and corresponding meanings of parameters. **B.** Equivalent schematic diagram of the contact area between carbon fiber bundles in mutual contact.

In the initial state (k = 0), volume (V) and the width (b) of the contact part of the carbon fiber bundle were constant, and the resistance was R_0 at this time. After bending, the resistance decreased to R_1 due to the quantum tunneling and the change of the contact area. The relationship between the resistance of the contact part of the carbon fiber bundle and the contact area was shown in Equation (1) as a preconditioner.

$$\begin{cases} R = \dfrac{\rho h}{S} \\ V = Sh \end{cases} \tag{1}$$

where R was resistance (Ω). ρ was the resistivity of the material (Ω-m). h was the length or thickness of the material (m). S was the cross-sectional area of the material (m²). V

was the volume (m^3). Then equation was obtained as follows.

$$R_0 S_0^{\ 2} = R_1 S_1^{\ 2} \tag{2}$$

where S_0 and S_1 were the contact area before and after bending, respectively, reflecting the quantitative relationship between the resistance of the contact portion of the carbon fiber bundle and the square of the contact area before and after bending. The area of the carbon fiber bundle in the contact part was calculated as shown in Equation (3).

$$\begin{cases} S_0 = (\pi + \theta_0) rb \\ S_1 = (\pi + \theta) rb \end{cases} \tag{3}$$

where θ_0 was the initial contact angle. r was the radius of the carbon fiber bundle. b was the width of the carbon fiber bundle. θ was the new contact angle after bending. The vertical height of the carbon fiber bundle at different contact angles was shown in Equation (4).

$$\begin{cases} h_0 = \dfrac{V}{(\pi + \theta_0) rb} \\ h_1 = \dfrac{V}{(\pi + \theta) rb} \end{cases} \tag{4}$$

where h_0 was the vertical height of the carbon fiber bundle in the initial state (unbent). h_1 was the vertical height of the contact portion of the carbon fiber bundle after bending.

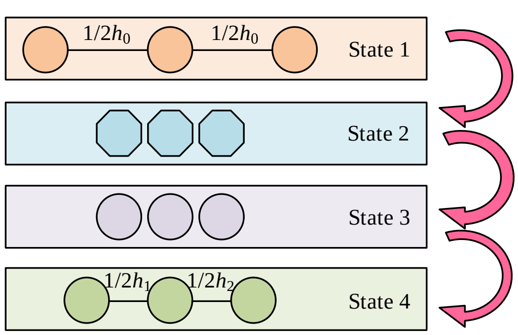

Figure 4. Schematic diagram of the decomposition of the interaction between two influencing mechanisms.

The decomposition of the interaction of the two influence mechanisms was shown in Figure 4. The change in sensor resistance was determined by a combination of bending-induced contact area changes and QTEs. These effects were more pronounced under different bending conditions of the carbon fiber bundle.

Design of high-sensitivity flexible bending sensor based on motion monitoring

Finger movements are crucial, and their joints have a wide range of motion that covers the possible flexion angles of almost all joints in the human body. Thus, tracking and digitizing finger joint movements can offer crucial data assistance for motion monitoring in addition to improving the understanding of hand function. In this study, the sensor was located at the joint part of the index finger to capture the degree of bending of the finger joint during movement. The fingers were bent at different angles of 30°, 90°, and 110° to collect single-channel data. Strain factor was a key indicator of sensor sensitivity, which represented the rate of change between the sensor output (resistance or capacitance change) and the strain applied and was shown in equation (5).

$$GF = \frac{(\Delta R / R_0)}{|\varepsilon|} \tag{5}$$

where *GF* was the measurement coefficient. ΔR was the variation in the sensor's resistance prior to and following strain. R_0 was the sensor's resistance in the absence of tension. $|\varepsilon|$ was the ratio of the change in material length to the original length. During the preparation of the high-sensitivity flexible bending sensor, special attention was paid to the size of fingers to ensure the fit and comfort of the sensor to the finger joints. The sensors consisted of three independent units and mounted at three key joint locations including the metacarpophalangeal joint (unit 1), the proximal interphalangeal joint (unit 2), and the distal interphalangeal joint (unit 3). Since unit one needed to cover the larger movement area of the

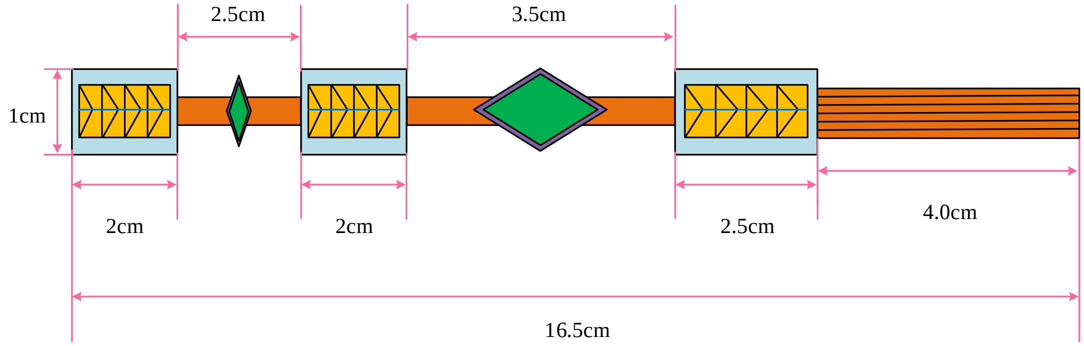

Figure 5. Schematic diagram of flexible sensor design for index finger.

metacarpophalangeal joint, its length exceeded that of units two and three to ensure that the sensor could comprehensively capture the movement changes of the joints. The flexible sensor design for the index finger consisted of multiple connecting sections located between the metacarpophalangeal, proximal, and distal phalangeal joints. The length of the reserved flexible circuit board could be adjusted according to the length of the individual finger to ensure precise positioning and natural bending of the sensor during application. The diamond-shaped structure with a hollowed-out center allowed the wires to deform with the bending of the finger, significantly improving the sensor's tensile properties, which prevented the sensor from breaking due to the slight stretching of the skin surface, ensuring its durability and long-term reliability (Figure 5).

Experimental test of designed sensors

A total of 10 healthy volunteers with 4 males and 6 females aged from 22 - 35 years old were recruited to participate in the validation experiments. All subjects signed informed consent form, and a medical examination confirmed the absence of any neuromuscular disease or joint injury affecting finger motor function. The sensors were individually attached to the three main joint locations of the subject's index finger and their response data were recorded under the standard movement paradigm. The procedures were approved by the IRB committee of Anhui Technical College of Mechanical and Electrical Engineering, Wuhu, Anhui, China. The designed sensor was evaluated by characterizing the stress response under different bending angles. Briefly, the sensor was attached to the index finger of a mechanical test rig to simulate human joint motion. Three typical bending angles of 30°, 60°, 90° were selected based on clinical finger movement ranges. For each angle, cyclic bending tests were performed at a frequency of 0.5 Hz for 10 cycles using TH-5806 wire bending testing machine (Suzhou Tuobo Machinery Equipment Co., Ltd., Suzhou, Jiangsu, China) with voltage signals recorded continuously using a Keysight 34461A digital multimeter (Keysight Technologies, Santa Rosa, CA, USA). The signals were processed using a 5th order Butterworth low pass filter with the cutoff frequency of 10 Hz to filter noise. Further, two circuit connections of forward and reverse were set up. The voltage changes of the flexible sensor were then recorded during the application and removal of pressure. The sensor's output voltage signal was monitored on the time axis in each connection mode. The pressure cycling tests were performed using a Zwick/Roell Z010 universal testing machine (Ulm, Germany) with a 50 N load cell, 0 - 5 kPa dynamic pressure at 1 Hz frequency. Stress signals were recorded at 1,000 samples/second and analyzed using MATLAB R2023a software (MathWorks, Natick, MA, USA).

Results and discussion

Voltage response characteristics at different bending angles

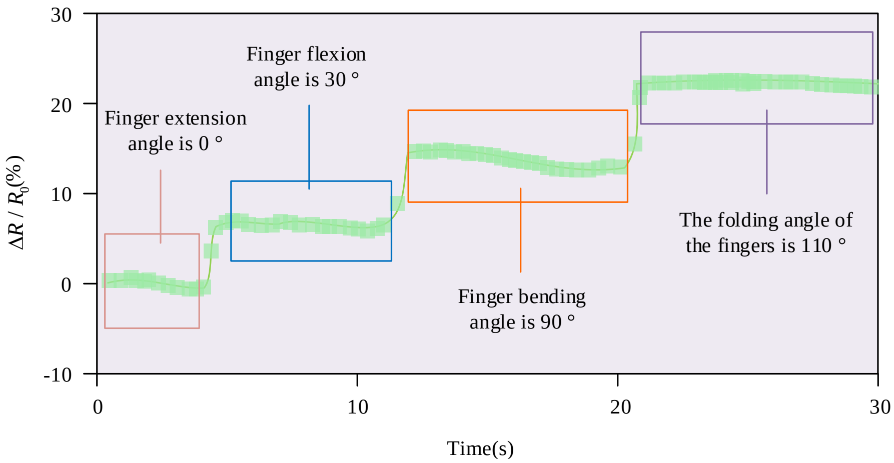

Figure 6. Relationship between the bending angle of the index finger joint and the change in sensor resistance.

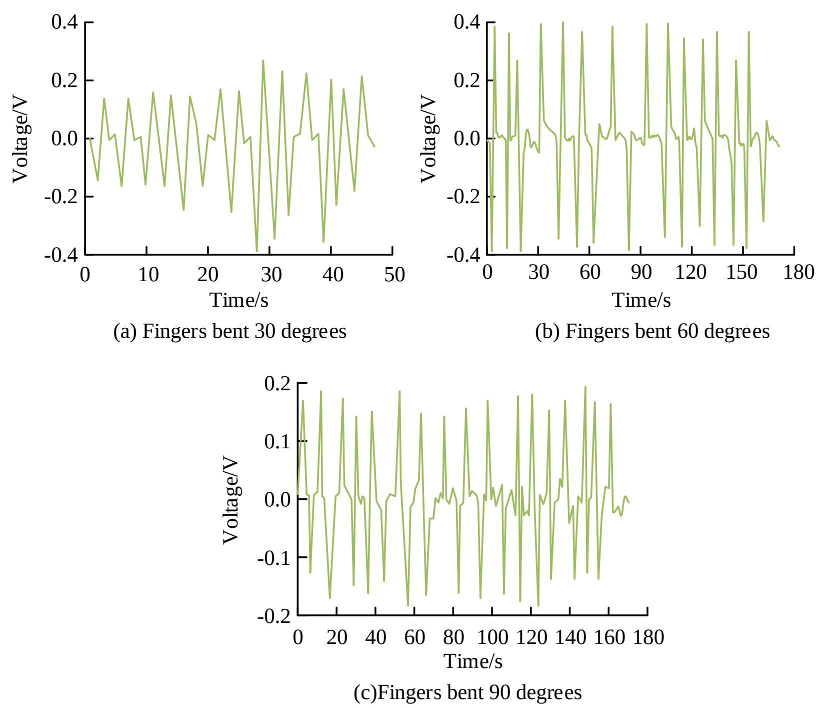

Figure 7. Schematic diagram of voltage response of flexible sensor under different finger bending angles.

The resistance changes of the sensors all exhibited a consistent rising trend as the finger's bending angle increased from 0° (completely extended) to 110° (maximum bending) (Figure 6). The results indicated that the sensor could track the finger's movements in real time. At specific angles such as 30°, 60°, and 90°, the changes of resistance values were more obvious, which reflected the high sensitivity and responsiveness of the sensor and indicated that the sensory could accurately reflect the motion state of the finger and the dynamic activity of the joint. The voltage responses of the flexible sensors at different finger bending angles demonstrated that the change of flexible sensor voltage signal when the finger was bent at 30 degrees showed a slight fluctuation (Figure 7a), which suggested that the flexible sensor could precisely record the

Table 1. Voltage output characteristics of flexible sensors under different pressure conditions.

Pressure type	Pressure amplitude (kPa)	Duration (s)	Output voltage (V)	Fluctuation amplitude (V)	Noise transmission rate (V)	Linear responsiveness (V/kPa)	Overall signal stability
Static	0.1	30	0.00238	0.00043	0.00007	0.0238	0.976
Static	0.5	30	0.00471	0.00079	0.00014	0.0094	0.972
Dynamic	1.0	30	0.00833	0.00165	0.00019	0.00833	0.948
Dynamic	2.0	30	0.01162	0.00201	0.00023	0.00581	0.935
Dynamic	3.0	30	0.01620	0.00253	0.00031	0.00540	0.925
Static	5.0	60	0.02385	0.00307	0.00048	0.00477	0.915
Dynamic	4.0	30	0.01987	0.00289	0.00035	0.00497	0.910

minute motions of the finger when it was slightly bent. Although accompanied by a certain amount of noise, it still demonstrated its sensitivity to low intensity bending. When the finger was bent at 60 degrees, the signal showed a more pronounced fluctuation, indicating a more significant response of the flexible sensor at moderate bending angles (Figure 7b), while the finger was bent at 90 degrees, the signal fluctuations were obvious, more frequent, and larger in amplitude, indicating that the sensor could respond quickly to the dynamic changes of the finger under high bending conditions (Figure 7c). The flexible sensor's voltage output characteristics under various pressure application scenarios showed that, at static pressure, the output voltages were 0.00238 V and 0.00471 V for 0.1 kPa and 0.5 kPa, respectively, while the dynamic pressures were 0.00833 V and 0.01162 V for 1.0 kPa and 2.0 kPa, respectively (Table 1). As the pressure amplitude increased, the output voltage and fluctuation amplitude tended to increase while the linear response decreased. The results suggested that the sensor's sensitivity to variations in pressure declined. The noise transmission rate increased slightly, but overall signal stability remained at a high level. In particular, the signal stability was 0.915 at a static pressure of 5.0 kPa, while it was 0.910 at a dynamic pressure of 4.0 kPa. The results showed that the sensor maintained a relatively stable performance under different pressure conditions.

Effect of circuit connection polarity

The results of sensitivity and stability analysis showed that the voltage signal change of the flexible sensor in the positive connection circuit showed obvious signal voltage fluctuations during the pressure application and removal process, and multiple sharp peaks and drops appeared during the pressure application process, which confirmed the sensor's fast and sensitive response to external pressure. The obvious voltage changes characteristics showed the good responsiveness of the flexible sensor to effectively detect small pressure changes (Figure 8a). The voltage signaling of the flexible sensor in the reverse connection circuit also displayed the voltage fluctuations when pressure was applied and removed (Figure 8b), but the magnitude of the fluctuations and the pattern of changes were different compared to that shown in Figure 8a, which might be because it was related to the change in current direction and its effect on the internal circuitry of the sensor. The reverse connection condition led to a change in the peak position and amplitude of the signal, which affected the metrological characteristics of the sensor. The flexible sensor's partial output voltage responded under certain circumstances as a continuous cycle of voltage output, in which no external pressure was applied (Figure 8c). The signal cycle reached 20, 000 cycles, reflecting the stability and consistency of the sensor over a long period of operation. The uniformity and repeatability of the output signal indicated that the sensor had good long-term operational performance and its ability to maintain a consistent level of voltage output over multiple

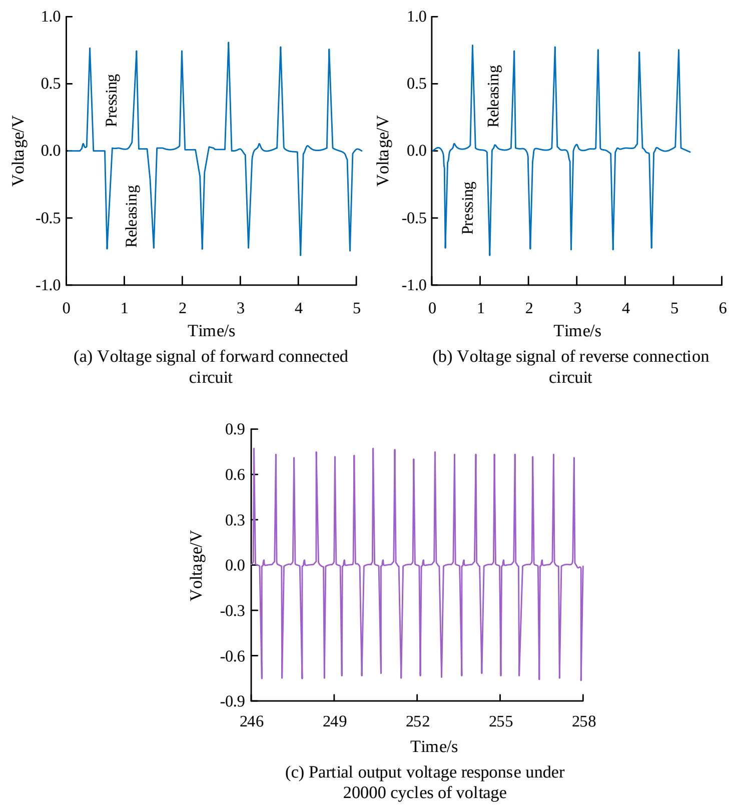

Figure 8. Analysis of voltage response characteristics of flexible sensors under different circuit connections.

Table 2. Sensitivity evaluation of flexible bending sensor in motion monitoring.

Applied Strain (°)	Output voltage change (V)	Sensitivity (V/°)	Response time (ms)	Repeatability standard deviation (V)	Sensitivity stability (%)
0.5	0.00087	1.74	120	0.00005	98.50
1.0	0.00195	1.95	115	0.00008	98.30
1.5	0.00320	2.13	110	0.00012	97.80
2.0	0.00459	2.30	105	0.00009	98.10
2.5	0.00578	2.31	100	0.00011	97.50
3.0	0.00718	2.39	95	0.00006	98.80
3.5	0.00854	2.44	90	0.00010	98.60
4.0	0.01002	2.50	85	0.00015	97.20

uses while ensuring high sensitivity of the instrument. The sensitivity of flexible bending sensors in motion monitoring showed that, as the strain increased, the output voltage change increased from 0.00087 V to 0.01002 V, and the sensitivity fluctuated between 1.74 and 2.50 V/°. The response time decreased gradually from 120 ms to 85 ms. The repeatability standard deviation was between 0.00005 V to 0.00015 V, showing good repeatability. The sensitivity stability was maintained between 97.20% to 98.80%, which showed that the sensor had high stability and reliability under different strain conditions (Table 2).

Dynamic response in human motion monitoring

The voltage response of flexible sensors under different pressure loads showed that, when the

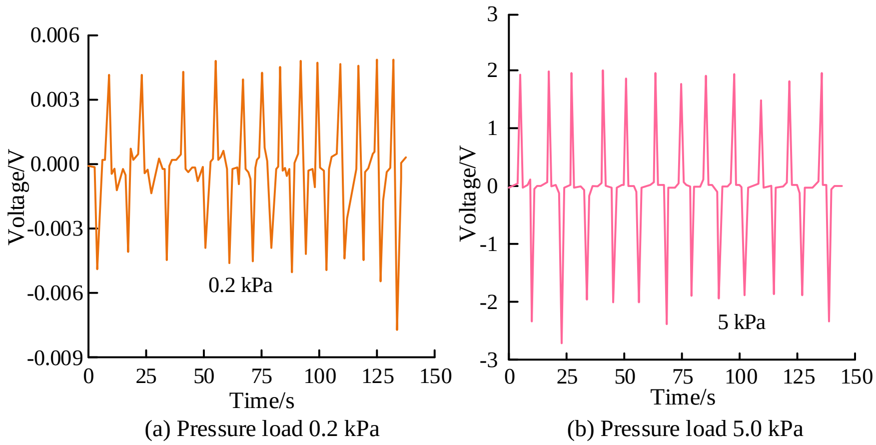

Figure 9. Voltage response characteristics of flexible sensor under different pressure loads.

Table 3. Voltage response characteristics of flexible sensor in motion monitoring.

Activity type	Applied load (kg)	Measurement duration (s)	Output voltage (V)	Fluctuation amplitude (V)	Response time (ms)	Average voltage (V)	Voltage standard deviation (V)
Walking	0.5	30	0.00357	0.00076	150	0.00320	0.00018
Running	1.2	30	0.00765	0.00110	140	0.00650	0.00035
Cycling	1.0	30	0.00543	0.00095	130	0.00480	0.00022
Jumping	0.8	30	0.01021	0.00200	120	0.00900	0.00050
Stair climbing	1.5	30	0.01289	0.00240	115	0.01150	0.00055
Strength training	2.0	30	0.01575	0.00290	110	0.01400	0.00048
Gymnastics	0.6	30	0.00652	0.00133	125	0.00590	0.00025

pressure load was 0.2 kPa, the voltage signal demonstrated small fluctuations, and the overall range of variation was relatively smooth, indicating that the sensor was relatively less sensitive to low pressure (Figure 9a). These small fluctuations were due to external influences or noise, implying that the output of the sensor was more steady state in a weak pressure environment. In addition, the small changes in signals still indicated that the sensor could capture small changes at low intensity pressures. However, the overall responsiveness and linearity of the relationship might be limited. The voltage signal under a pressure load of 5.0 kPa showed that the amplitude of the sensor's output voltage fluctuation increased significantly, and the overall signal variation region extended significantly (Figure 9b), which indicated that the flexible sensor's sensitivity was significantly improved under high pressure and was able to respond more effectively to the applied pressure changes. The frequent signal pulses reflected the rapid response of the sensor to dynamic pressure changes, which was due to the enhanced stretching of the sensor material properties under high pressure. This study investigated seven types of activities including walking, running, cycling, jumping, stair climbing, strength training, and gymnastics. The applied loads ranged from 0.5 to 2.0 kg, and the measurement duration was 30 s. The results showed that the output voltages were 0.00357 V, 0.00765 V, 0.00543 V, 0.01021 V, 0.01289 V, 0.01575 V, and 0.00652 V during walking, running, cycling, jumping, stairs climbing, strength training, and gymnastics, respectively, while the fluctuation amplitude, response time, average voltage, and voltage standard deviation also various with the types of activities, indicating the performance changes of the sensor under different dynamic conditions (Table 3).

Conclusion

This study proposed a novel highly sensitive flexible bending sensor based on PI/PA composite encapsulation for human motion monitoring applications. The sensor was fabricated using a simple hot-pressing technique with PA adhesive, which ensured robust mechanical stability and conformal contact with the skin. By interfacing carbon fiber bundles, the sensor achieved sub-degree resolution of 0.5° and fast dynamic response, demonstrating reliable detection of finger joint motion over a wide range of motion amplitudes. The PI/PA composite structure also demonstrated excellent mechanical durability, maintaining resistance stability within ±2 Ω after 20 cycles of 110° bending, confirming its suitability for long-term wearable use. The sensor's lightweight design and environmental durability make it ideal for healthcare monitoring and human-computer interaction. Future research will focus on multi-functional integration, durability testing under extreme conditions, and clinical validation to expand its practical utility.

References

1. Kong M, Yang M, Li R, Long YZ, Zhang J, Huang X, *et al*. 2024. Graphene-based flexible wearable sensors: Mechanisms, challenges, and future directions. Int J Adv Manuf Technol. 131(5):3205-3237.
2. Masoumian Hosseini M, Masoumian Hosseini ST, Qayumi K, Hosseinzadeh S, Sajadi Tabar SS. 2023. Smartwatches in healthcare medicine: assistance and monitoring: A scoping review. BMC Med Inform Decis Mak. 23(1):248-274.
3. Liang C, Sun J, Liu Z, Tian G, Liu Y, Zhao Q, *et al*. 2023. Wide range strain distributions on the electrode for highly sensitive flexible tactile sensor with low hysteresis. ACS Appl Mater Interfaces. 15(12):15096-15107.
4. Fu Z, Sajad A, Errington SP, Schall JD, Rutishauser U. 2023. Neurophysiological mechanisms of error monitoring in human and non-human primates. Nat Rev Neurosci. 24(3):153-172.
5. Wang Z, Ding J, Guo R. 2023. Printable all-paper pressure sensors with high sensitivity and wide sensing range. ACS Appl Mater Interfaces. 15(3):4789-4798.
6. Zhao R, He Y, He Y, Li Z, Chen M, Zhou N, *et al*. 2023. Dual-mode fiber strain sensor based on mechanochromic photonic crystal and transparent conductive elastomer for human motion detection. ACS Appl Mater Interfaces. 15(12):16063-16071.
7. Yang C, Wang W, Zhang B, Liu W, Zhang H, Zhang D. 2024. High sensitivity $SnSe_2$/MWCNTs flexible pressure sensors based on a lotus leaf biomimetic microstructure for electronic skin. J Mater Chem C. 12(28):10669-10677.
8. Xi G, Zhang D, Tang M, Zhang H, Sun Y, Zhang Y, *et al*. 2024. Fast-response, high-sensitivity multi-modal tactile sensors based on PPy/Ti_3C_2Tx films for multifunctional applications. Nano Res. 17(5):4410-4419.
9. Pan T, Yu Z, Huang F, Yao H, Hu G, Tang C, *et al*. 2023. Flexible humidity sensor with high sensitivity and durability for respiratory monitoring using near-field electrohydrodynamic direct-writing method. ACS Appl Mater Interfaces. 15(23):28248-28257.
10. Wang YF, Yoshida A, Takeda Y, Sekine T, Kumaki D, Tokito S. 2023. Printed directional bending sensor with high sensitivity and low hysteresis for human motion detection and soft robotic perception. Sensors (Basel). 23(11):5041-5053.
11. Ying S, Li J, Huang J, Zhang JH, Zhang J, Jiang Y, *et al*. 2023. A flexible piezocapacitive pressure sensor with microsphere-array electrodes. Nanomaterials (Basel). 13(11):1702-1714.
12. Gong YJ, Li ZG, Chen H, Guo TM, Gao FF, Chen GJ, *et al*. 2023. High power density energy harvesting and human motion monitoring with TMCM-$CdCl_3$/polymer composite. Matter. 6(6):2066-2080.
13. Park SJ, Kim J, Chu M, Khine M. 2023. Highly flexible wrinkled carbon nanotube thin film strain sensor to monitor human movement. Adv Mater Technol. 1(2):1600053-1600053.
14. Li Y, Yao M, Luo Y, Li J, Wang Z, Liang C, *et al*. 2023. Polydopamine-reinforced hemicellulose-based multifunctional flexible hydrogels for human movement sensing and self-powered transdermal drug delivery. ACS Appl Mater Interfaces. 15(4):5883-5896.
15. Lu D, Liao S, Chu Y, Cai Y, Wei Q, Chen K, *et al*. 2023. Highly durable and fast response fabric strain sensor for movement monitoring under extreme conditions. Adv Fiber Mater. 5(1):223-234.
16. Li J, Yin J, Wee MGV, Chinnappan A, Ramakrishna S. 2023. A self-powered piezoelectric nanofibrous membrane as wearable tactile sensor for human body motion monitoring and recognition. Adv Fiber Mater. 5(4):1417-1430.
17. Dornelas RS, Lima DA. 2023. Correlation filters in machine learning algorithms to select demographic and individual features for autism spectrum disorder diagnosis. J Data Sci Intell Syst. 3(1):7-9.
18. Zheng S, Chen X, Shen K, Cheng Y, Ma L, Ming X. 2024. Hydrogen bonds reinforced ionogels with high sensitivity and stable autonomous adhesion as versatile ionic skins. ACS Appl Mater Interfaces. 16(3):4035-4044.